Rocket Propulsion Laboratory

Swirl Coaxial Injector Design Packet

Aiden Lin, Andrew Furst, Ken Kuboshima, Rajveer Oberoi, Steven Nguyen

April 10, 2021

Contents

1 Documents

1.1 Executive Summary

The swirl coaxial injector has been an injection method of interest for liquid rocket engines (LREs) for decades mainly due to their reduced complexity in their designs and their high performance. Many research studies have been performed on swirl injectors that concentrates on discharge coe cient, spray cone angle, lm thickness, drop size, mixing, and dynamics under various test conditions. The objective of this paper is to document the design process and the analysis of a test-ready, LOx/methane, coaxial swirl injector prototype that uses UCSB RPL's LRE design constraints and the research discussed in rocketry literature.

1.2 Introduction and Target Specifications

The injector is the last component of a LRE before propellants are discharged into a combustion chamber. The pressurized liquid methane and oxygen must pass through the injector which disintegrates the liquids into combustible mist. Typically, three primary injection methods are used in LREs (e.g., jet-impinging, pintle, coaxial). The injection method that exceeds other methods in performance, stability, and versatility is the coaxial injector. More speci cally, a swirl-axial injector creates aerosolized droplets of fuel from an inner swirl chamber and evenly distributes them outwards to collide with an annular oxidizer spray. The swirling process and the collision of the two streams will thoroughly atomize the propellants and mix them together for optimal combustion in the chamber. In order to properly design the injector, it is important to understand the target speci cations and goals for the design.

The main requirements for the injector are to thoroughly break up liquid propellants into small droplets, mix and distribute propellants in the desired mixture ratio, spray the propellants into the combustion chamber uniformly, and decouple the feed system from the pressure oscillations in the combustion chamber.

1.2.1 Atomization

The primary function of an injector is to provide e cient combustion through atomization of the propellants. During the atomization process, the liquid propellant will be turned into much smaller droplets, facilitating the evaporation of propellants which leads to a more stable and e cient combustion process that is able to provide thrust without damaging the hardware [18].

According to Gontijo, Fischer and Costa's paper on evaluation of SMD e ect [19], SMD is one of the most important factors a ecting the performance of an injector; a smaller SMD would allow the chamber pressure and correspondent pressure drop to be larger. A coaxial swirl injector, compared to many other types of injectors, is known for having advantages of superior atomization and mixing characteristics. A coaxial swirl injector completes the atomization process through the interaction and collision between a swirling conical and annular cylindrical liquid sheets within the chamber [20]. The resulting droplets from this process will have small Sauter mean diameters (SMD), which allows the coaxial swirl injector to yield e cient atomization within a proportionally small volume. For example, another popular injector design, the pintle injector, often has an SMD of 100 to 600 micrometers based on designs and parameters [21] [22] while coaxial swirl injectors often has an SMD that is smaller than

200 micrometers [23] [24]. fter considering atomization e ciency, the coaxial swirl injector was chosen to be the type that this design uses.

1.2.2 Flow Rate, Mixture Ratio, and Flow Uniformity

For optimal combustion, the injector should spray the LOx and the LCH4 at a mixture ratio of 2.8 and a total mass ow rate of 2.7 $\frac{lbm}{s}$. Knowing these two constraints, the LOx must have a mass ow rate of 2.0 $\frac{lbm}{s}$, and the LCH4 must have a mass ow rate of 0.7 $\frac{lbm}{s}$.

1.2.3 Spray Angle and Spray Uniformity

This section will talk through the spray angle and how 45 degrees is a good target angle that utilizes the combustion chamber volume for maximum atomization. Spray uniformity quanti ed by volume fraction and SMD.

1.2.4 Pressure Decoupling

As the propellants combust in the combustion chamber, pressure oscillations can potentially lead to acoustic combustion instability if the oscillations make their way into the feed system. One method to combat this issue is to create a su cient pressure drop across the injector which acts as a bu er between the pressure oscillations of the combustion chamber and the sensitive feed system.[17]. However, this pressure drop cannot be so high that it would pose unnecessarily high stress on the injector. According to the recommendations of (ROCKET LAB PAPER), a pressure drop of approximately 70 to 150 psi is appropriate for small, liquid-fuel rocket engines. It is also know that the experiments that were done to test equation (4) used injection pressures of around 100 psi, or 0.69 MPa [16], so it was decided that 0.69 MPa as an appropriate pressure drop across the injector.

2 Design and Analysis

2.1 Fuel Flow Geometry Design

2.1.1 Governing Parameters

This section will de ne important geometric parameters that will characterize the swirl ow of the fuel. ($\dot{m}$; P; A_p; D_0; D_s; K; C_d; X). In order to characterize the ow using the geometry, it's important to understand some key dimensions and parameters that are most in uential. The most commonly studied injector parameters were the inlet area, A_p, the swirl diameter, D_s, and the nozzle diameter, D_0. The two diameters are labeled in gure 1a, while inlet area can be calculated by multiplying the number of inlets by the area of each one. Generally, the subscripts s and 0 refer to dimensions relating to the swirling section and the nozzle section respectively. From these 3 main parameters, a dimensionless parameter that is often used in swirl literature, K, can be de ned as: $K = \frac{A_p}{D_s D_0}$.

Outside of geometric parameters, there are also parameters dedicated to characterizing the ow that should be mentioned. When the injector is in operation and uid is swirling, an air core often forms because of the pressure distribution inside the injector. This air core can be visualized as in gure 1b. This air core is normally modeled using the variable X (which shall be referred to as the passage emptiness coe cient), representing the area at the ori ce lled with air divided by the total

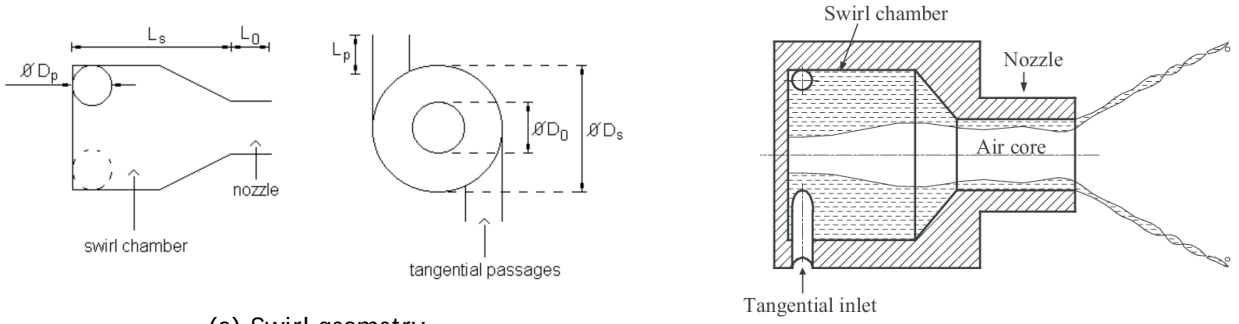

(a) Swirl geometry

(b) Air core

Figure 1: Important characteristics of swirl injectors

area of the ori ce. Another important ow characteristic is the discharge coe cient, C_d, representing the losses that occur within the injector. The discharge coe cient helps to show how the mass ow rate through the injector compares to theoretical ow.

2.1.2 Governing Equations

It is de ned with equation (1), with A_0 representing the ori ce area, as the density, and P as the pressure drop across the injector. $\dot{m}$ is the mass ow rate, as calculated earlier.

$$C_d = \frac{\dot{m}}{A_0\sqrt{2 \quad P}} \tag{1}$$

In a study by researchers Gi en and Muraszew [16], they were able to de ne discharge coe cient as a function of the passage emptiness coe cient:

$$C_d = 1{:}17\sqrt{\frac{(1-X)^3}{1+X}} \tag{2}$$

A separate study by Rizk and Lefebvre [15] found a di erent equation that also worked well for predicting the discharge coe cient:

$$C_d = 0{:}35\,(K)^{0:5}\,(\frac{D_s}{D_0})^{0:25} \tag{3}$$

These two experimental equations for the discharge coe cient were combined in a paper by Lefebvre and Suyari to yield an equation that successfully predicts the passage emptiness coe cient as a function of the swirl geometry [16]:

$$0{:}0894879\,(K)\,(\frac{D_s}{D_0})^{0:5} = \frac{(1-X)^3}{1+X} \tag{4}$$

Lastly, the spray angle was one of the most important design constraints. A study by Gi en and Muraszew [15] used all the parameters above to predict the spray angle in equation (5). The angle is measured from a centerline through the injector, to the outer spray of the liquid sheet.

$$sin(\ ) = \frac{C_d}{2\,K\,(1+\sqrt{X})} \tag{5}$$

2.2 Oxidizer Flow Geometry Design

2.2.1 Governing Parameters

This section will de ne important geometric parameters that will characterize the axial ow of the oxidizer. As mentioned previously, the target ow conditions of the outer oxidizer ow includes delivering the correct mass ow rate (m_{ox} = 0:9008kg=s), and producing a su cient pressure drop across the ow channel (P_{ox} = 0:69MPa). We assume that the uid is incompressible, therefore making density constant ($_{ox}$ = 998kg=s). Thus, according to equation (1), the remaining parameters that must be considered are the annular exit area (Ao_{ox}) and the discharge coe cient (Cd_{ox}). The annular exit area can be increased or decreased to adjust the exit ow velocity. This comes in handy when predicting the impinging spray angle.

2.3 Matlab Implementations

While the outer ow of LOX is simple to characterize, the inner swirl presents a much more complex problem, as evidenced by the ow theory. In order to visualize the di erent relationships between geometric parameters and how each played a role in a ecting the swirl characteristics, we used Matlab. As outlined earlier, the 3 de ning geometric parameters are the swirl chamber diameter, D_s, the nozzle diameter, D_0, and the inlet area, A_p. We were able to calculate spray angle, pressure drop, and other relevant parameters for di erent combinations of these 3 dimensions.

One of the rst plots we made was meant to study the relationship between pressure, P, and dimensionless parameters K and X (gure 2a). It is recommended to design for a K in a range of 0.19 to 1.21 [15], which we con rmed by plotting a surface relating those three variables. To make this plot, we used the `meshgrid()` and `surfc()` functions. During this initial script, we set a constant value for the inlet area and varied the swirl and nozzle diameters. After setting a range of dimensions for D_s and D_0, the `meshgrid()` function created 2-dimensional matrices for each variable that allowed us to consider each possible combination of the dimensions. Using those matrices, the `surfc()` function plotted a three dimensional surface relating the pressure, K value, and X values corresponding to each combination of dimensions. As can be seen in gure 2a, the `surfc()` function also adds contour lines that can be seen on the xy plane.

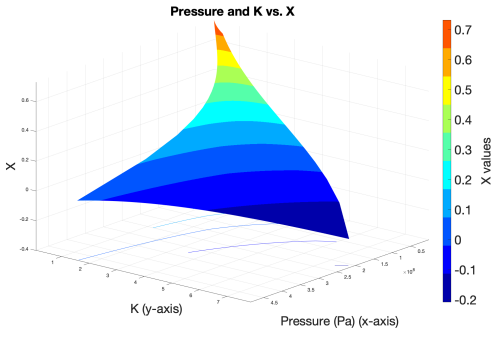

(a) Relationship between P, K, and X for constant inlet area and varying swirl/nozzle diameters

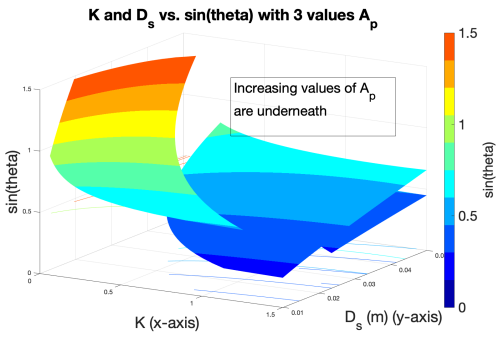

(b) Injector dimensions vs. spray angle

Figure 2: Visualizing relationships between ow characteristics and injector geometry

The color map shows that for certain values of K and P, the X value is negative. This doesn't make sense, so we assumed this is representative of the regions where the experimental equations do not accurately model the swirl. Using the contour lines and knowing that we would prefer a high pressure, the upper limit for K is approximately 1.5. This is slightly different from the [15] paper recommendation, but that could be due to different injection pressures.

Next, we wanted to calculate the spray angle as well as capture the effect of changing the inlet area. We continued using `meshgrid()` to account for the different combinations of dimensions, and chose three constant values of A_p to calculate. Figure 2b shows the results, and we can see that for smaller values of A_p, the spray angle seemed to increase with our given set of dimensions. There's a region of the graph colored yellow to red that is labeled $sin(\ ) > 1$. This doesn't make sense, so we assumed this was a regime where the experimental equations are not accurate.

On figure 2b, the 3 different A_p angles make up the three different surfaces that are shown. Larger values of A_p seemed to have the effect of decreasing the spray angle, as those larger values correspond to the surfaces that are lower on the spray angle axis. These results confirmed that a large range of spray angles could be achieved in our range of data, and also suggests that the effects of inlet area should be taken into account more carefully.

In order to take into account the effects of three independent dimensions on spray characteristics, we looked into Matlab's isosurface capabilities. Using `isosurface()`, we were able to plot combinations of points where the spray angle is a certain desired angle (for this graph, we chose an arbitrary 48 degrees), along axes of D_s, D_0, and A_p. This is shown in figure 3a. The isosurface was colored using `isocolors()` to visualize the pressure along the surface, so we can find points with a desirable spray angle and injection pressure. Along the right edge, where D_0 values are low, the surface has strange behavior where it is not smooth and has what looks like creases. This is likely because, as we saw on figure 2a, there are certain ranges of X where it is negative. In order to calculate equation (5), we needed to take the absolute value of X to avoid the negative values. We came to the conclusion that this looks like a regime where the experimental equations do not accurately model the flow characteristics.

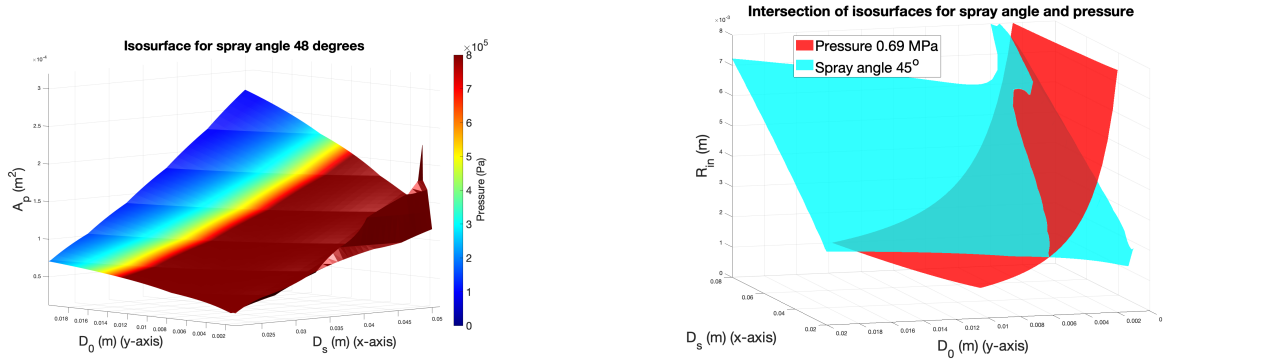

(a) Isosurface where spray angle is 48 degrees

(b) Intersection of isosurfaces for spray angle 45 degrees and pressure 0.69 MPa

Figure 3: Implementations of isosurfaces

However, for a more accurate method, we wanted to be able to find specific points that could satisfy both our constraints for spray angle and injection pressure without hand-picking points along

a 3D surface. Due to the form of equation (4), we couldn't find a way to solve directly for the points that could satisfy a pressure constraint and a spray angle constraint by hand. Instead, we returned to Matlab and developed a method for finding the intersection of two isosurfaces. First, we plotted an isosurface for spray angle and injection pressure together in figure 3b. Similar to in figure 3a, there's a region along the spray angle isosurface where the surface has strange behavior and the experimental equations we are using may be inaccurate. However, there seem to be intersections between the two surfaces that do not fall in that region.

To find these points, we used `patch()` to extract face and vertices data from the `isosurface()` function. We wrote a function to take in that face and vertices data and check for points that were shared between the two surfaces. Since there are some points that do not line up perfectly, but are very close to each other, the code was designed to find points within a small tolerance of each other. Using this, we were able to find points that could satisfy both the constraint of a 0.69 MPa injection pressure and a 45 degree spray angle. After determining these values, the next step was to simulate this injector design using ANSYS Fluent.

3 Manufacturing

3.1 Introduction

Numerous manufacturing techniques were considered while designing and prototyping the injector and several were selected as possible candidates for actual production.

3.2 Machining

Machining the injector greatly limits the inner complexity and increases the part count of the injector. This multi-part design necessitates not only tight mating tolerances to maintain concentricity of the inner and outer swirl chambers, but also seals capable of withstanding the moderately high pressure and the low temperatures (-315°F [1]). O-rings constructed from low temperature PTFE with a percent squeeze of 20% was selected for all radial static seals to prevent leaking of fuel or oxidiser after the injector has been chilled to operating temperature. Mating surfaces of the injector parts must be machined to a RC4 sliding clearance fit (±0.002") with critical inner diameters being -0,+0.002 and critical outer diameters being +0,-0.002 to allow for easy assembly and maintain concentricity [2]. Machining the injector allows for almost unlimited material choice, including acrylic for flow testing, aluminium for easy manufacturing, and stainless steel or inconel for final production.

Compared to other manufacturing techniques machining has a long lead time as each part must be machined or programmed individually and due to the nature of removing material raw material costs are typically higher then other methods. Outsourcing the machining would require perfect engineering drawings and good communication with the manufacturer on critical tolerances and fitment. Machining could be done in house which could eliminate labor cost, however it would limit geometry to that which could be constructed on a vertical CNC mill and manual lathe. Should the part be outsourced it should ideally be manufactured by a single source to allow for a dry fit up to insure part compatibility before being shipped out.

3.3 Direct Metal Laser Sintering (DMLS)

DMLS allows for the strongest additive manufactured single or multi part injector. The material choices for DMLS include a cheaper 6005 series aluminum, two di erent avors of stainless steel, and inconel all with a shot blasted external (but not internal) nish [3]. Typical accuracy of DMLS prints are ±0.003"[4] however due to the uneven heating during the laser sintering process thin parts have a tendency to warp if unsupported. Inside surfaces can typically achieve a RA 15 um raw surface nish however surface nish decreases as the overhang angle decreases as measured from the horizontal[5]. DMLS machines require support when building any overhang less then 35 degrees from the horizontal, overhangs greater then 3-4 mm, and horizontal holes with a diameter of greater then 8mm [6]. DMLS support structure is constructed from build material, and must have the proper clearance to be removable after printing. Due to the layered nature of the deposition process, the yield stress depends on the orientation of the layer in regards to the principal stress. Under lab conditions yield stress parallel to principal stresses were found to typically be 80% less then their billet counterparts, and yield stress perpendicular to layer orientation resulted in 60% the yield stress of billet [13]. A stainless steel version of the injector will cost $2.3k with a lead time of two weeks, inconel quotes will likely be 1.5-2X the cost of SS [7].

3.4 Binder Jetting

Metal Binder Jetting has many advantages over other metal additive manufacturing methods such as DMLS in that it is much cheaper, faster, and requires less support material. Two di erent processes can be used to create binder jetted metal parts. The rst method takes a "green" or unsintered part from the printer and uses lower temperatures (aprox 100-200 degrees C) to burn away any uncured binder and sinter the part together creating a fragile 60% porous matrix "brown" part [8]. This porous matrix can than be in ltrated with a low melting point metal (typically a bronze alloy) to ll the voids left by the burned o binder creating a nal density of approximately 95% [9]. The second method takes the "brown" part and then resinters it at 1200-1400 degrees C to create a homogeneous part with 93-99% density. This second method has the advantage of being able to create a much stronger part at the expense of introducing 25-35% more shrinkage and distortion as the part sinters together [10]. Due to the high temperatures involved with metal 3D printing part shrinkage and warpage is unavoidable, but can be minimized by reducing thin sections, using consistent wall thicknesses, and through complex computer simulations to print the part to account for heat treat warping. A well designed part can typically hold tolerances of .004" and create surface nishes of RA 6 um [11]. The yield strength of a 316 stainless steel part with bronze in ltration typical demonstrates approximately the same yield strength as billet 316, however its ultimate yields strength is only 80% that of billet [14]. The cost for a steel part with bronze in ltration costs approximately $340 with a two week lead time [12].

3.5 Stereolithography (SLA)

Although not a production method for the nalized injector, SLA allows for quick and cheap local rapid prototyping of the injector in a clear resin. These prints would prove useful to verify simulation data during water ow tests as well as help with the calculations of the ow lm thickness.

References

[1] H. Alcaraz, M. Aslo, J. Button, M. Carmi, G. Clover, J. Dibachi, B. Dutcher, M. Li, N. McCarthy, D. Rogers, and C. Meng, \UCSB RPL Static Fire Design packet," UCSB RPL, 09-Jun-2020. [Online]. Available: https://www.rplatucsb.com/. [Accessed: 17-Apr-2021].

[2] E. Oberg and L. Brengelman, Machinery's handbook, 30th ed. South Norwalk, CT, U.S.A. : Industrial Press, Inc., 2020.

[3]

[4] Protolabs Inc. \Metal 3D Printing Design Guidelines." Design Guidelines: Direct Metal Laser Sintering (DMLS), Protolabs, www.protolabs.com/services/3d-printing/direct-metal-laser-sintering/design-guidelines/.

[5]

[6]

[7]

[8] \MIM process options ," Smith Metal Products, 02-Sep-2020. [Online]. Available: https://smithmetals.com/design-guide/process-options/sintering/. [Accessed: 17-Apr-2021].

[9] A. Varotsis, \Introduction to binder jetting 3D printing," 3D Hubs. [Online]. Available: https://www.3dhubs.com/knowledge-base/introduction-binder-jetting-3d-printing/. [Accessed: 17-Apr-2021].

[10] A. Huckstepp, \Metal Binder Jetting," Digital Alloys, 11-Jul-2019. [Online]. Available: https://www.digitalalloys.com/blog/binder-jetting/. [Accessed: 17-Apr-2021].

[11] A. Varotsis, \Introduction to binder jetting 3D printing," 3D Hubs. [Online]. Available: https://www.3dhubs.com/knowledge-base/introduction-binder-jetting-3d-printing/. [Accessed: 17-Apr-2021].

[12] what do you want a PDF?

[13] T. M. Mower and M. J. Long, \Mechanical behavior of additive manufactured, powder-bed laser-fused materials," Materials Science and Engineering: A, 10-Nov-2015. [Online]. Available: https://www.sciencedirect.com/science/article/pii/S092150931530530X. [Accessed: 17-Apr-2021].

[14] \316 Stainless Steel In ltrated with Bronze." ExOne Company, North Huntingdon, 31-Mar-2014.

[15] P. T. Lacava, D. Bastos-Netto, and A. P. Pimenta, "Design Procedure and Experimental Evaluation of Pressure-Swirl Atomizers," presented at 24^{th} Intl. Cong. of the Aeronautical Sciences, Brazil, 2004.

[16] M. Suyari and A. H. Lefebvre, "Film Thickness Measurements in a Simplex Swirl Atomizer," *Journal of Propulsion*, vol. 2, no. 6, November-December, 1986.

[17] T. Khil, Y. Chung, V. Bazarov, and Y. Yoon, "Dynamic Characteristics of Simplex Swirl Injector in Low Frequency Range," *Journal of Propulsion and Power*, vol. 28, no. 2, March-April 2012.

[18] Zhongtao Kang, Zhen-guo Wang, Qinglian Li, Peng Cheng, "Review on pressure swirl injector in liquid rocket engine, Acta Astronautica," Volume 145, 2018, Pages 174-198, ISSN 0094-5765. [Online]. Available: https://www.sciencedirect.com/science/article/pii/S0094576517316831. [Accessed: 12-May-2021].

[19] Gontijo, Maur cio & Alexandre Achilles Fischer, Gustavo Costa, Fernando. (2020). Evaluation of SMD E ects on Characteristic Lengths of Liquid Rocket Engines Using Ethanol/LOx and RP-1/LOx. 10.26678/ABCM.ENCIT2020.CIT20-0794.

[20] Calimanescu, Ioan. (2008). Numerical Investigation of Swirl Injector LOX/GH2 Ratio In uence over Combustion Conditions into a Liquid Rocket Engine.

[21] S. Ninish, Aravind Vaidyanathan, K. Nandakumar, Spray characteristics of liquid-liquid Pintle injector, Experimental Thermal and Fluid Science, Volume 97, 2018, Pages 324-340, ISSN 0894-1777, https://doi.org/10.1016/j.exptherm usci.2018.03.033.(https://www.sciencedirect.com/science/article/pii/S08

[22] Suji Lee, Daehwan Kim, Jaye Koo, Youngbin Yoon, Spray characteristics of a pintle injector based on annular ori ce area, Acta Astronautica, Volume 167, 2020, Pages 201-211, ISSN 0094-5765, https://doi.org/10.1016/j.actaastro.2019.11.008. (https://www.sciencedirect.com/science/article/pii/S0094576519313852)

[23] Han, Poong-Gyoo Seol, Jae-Hoon Hwang, Seong-Ha Yoon, Youngbin. (2003). The Spray Characteristics of Swirl Coaxial Injectors. 41st Aerospace Sciences Meeting and Exhibit. 10.2514/6.2003-490.

[24] Kamalakannan Kannaiyan, Manoj Venkata Krishna Banda, Aravind Vaidyanathan, Planar Sauter Mean Diameter measurements in liquid centered swirl coaxial injector using Laser Induced Fluorescence, Mie scattering and laser di raction techniques, Acta Astronautica, Volume 123, 2016, Pages 257-270, ISSN 0094-5765, https://doi.org/10.1016/j.actaastro.2016.03.011. (https://www.sciencedirect.com/science/article/pii/S0094576515302812)